

RSC Advances



This is an *Accepted Manuscript*, which has been through the Royal Society of Chemistry peer review process and has been accepted for publication.

Accepted Manuscripts are published online shortly after acceptance, before technical editing, formatting and proof reading. Using this free service, authors can make their results available to the community, in citable form, before we publish the edited article. This *Accepted Manuscript* will be replaced by the edited, formatted and paginated article as soon as this is available.

You can find more information about *Accepted Manuscripts* in the [Information for Authors](#).

Please note that technical editing may introduce minor changes to the text and/or graphics, which may alter content. The journal's standard [Terms & Conditions](#) and the [Ethical guidelines](#) still apply. In no event shall the Royal Society of Chemistry be held responsible for any errors or omissions in this *Accepted Manuscript* or any consequences arising from the use of any information it contains.

Label-Free and Turn-on Fluorescent Cyanide Sensor Based on CdTe Quantum Dots Using Silver Nanoparticles

Ali A. Ensafi*, N. Kazemifard, B. Rezaei

Department of Analytical Chemistry, College of Chemistry, Isfahan University of Technology, Isfahan 84156–83111, Iran

Abstract

Silver nanoparticles were used to develop a simple turn-on fluorescent assay based on glutathione-capped CdTe quantum dot for the determination of trace amounts of the lethal poison, cyanide. It was found that the fluorescence intensity of glutathione-capped CdTe quantum dot increased with increasing cyanide concentration. Several experimental variables such as pH, the amounts of quantum dots and silver nanoparticles were affect the analytical signals were optimized. Using this optical sensor under optimum conditions, cyanide was measured in the range of 0.01 – 2.5 $\mu\text{g mL}^{-1}$ with a detection limit as low as 0.004 $\mu\text{g mL}^{-1}$. Relative standard deviations of 2.0% (for 0.5 $\mu\text{g mL}^{-1}$, n=10) and 1.8% (for 2.0 $\mu\text{g mL}^{-1}$, n=10) were obtained. Investigation of the effects of potential interfering anions on the response of the sensor revealed the high selectivity of the sensor for the detection of cyanide in real samples. High sensitivity, superior selectivity, low detection limit (0.004 $\mu\text{g mL}^{-1}$) and ease of production are the most important advantages of the present sensor. Finally, the sensor was lucratively applied for the determination of cyanide in real samples.

Keywords: Cyanide, CdTe quantum dot, Silver nanoparticles, Turn-on fluorescent.

Corresponding author: Fax: +98–31–33912350; Tel.: +98–31–33913269; E-mail: Ensafi@cc.iut.ac.ir; Ensafi@yahoo.com.

28 1. Introduction

29 Quantum dots (QDs) are brightly luminescent semiconductor nanoparticles that have
30 found wide applications in bioanalysis and bioimaging in recent decades. This is due to
31 their unique photoproperties such as wide UV–Vis absorption spectrum and narrow
32 photoluminescence spectrum.¹ Compared to organic dyes, QDs have a brighter
33 fluorescence by about 10–20 times and a better photostability by 100–200 times.² A lot of
34 studies in a variety of fields have been devoted over decades for the interesting optical
35 properties of nanoparticles such as silver and gold nanoparticles (SNPs and GNPs,
36 respectively).³

37 Plasmon resonance absorptions of SNPs and GNPs have molar extinction
38 coefficients ($\sim 3 \times 10^{11} \text{ M}^{-1} \text{ cm}^{-1}$) that make them good energy acceptors so that they often
39 serve the role of quenchers in fluorimetric methods.^{4–8} The fluorescence of CdTe-QDs is
40 significantly reduced by SNPs to the extent that their self-quenching effect could be
41 eliminated.

42 Cyanide is one of the most lethal toxins; $300 \mu\text{g mL}^{-1}$ of this poison would be
43 enough to kill a man quickly. Cyanide's toxicity to humans lies in its ability to suppress
44 oxygen transfer via its binding to the active sites of cytochrome C oxidase that results in
45 hypoxic.⁹ Long-term exposure to low amounts of cyanide also affects the central nervous
46 system.¹⁰ Cyanide poisoning may also occur through inhaling emissions from residential
47 applications, metal plating, metal mining, plastic manufacturing, and metal processing
48 industries.¹¹

49 Several analytical methods have been developed for the detection of cyanide
50 including liquid chromatography-mass spectrometry,¹² fluorimetric^{13–15}
51 chemiluminescence,^{9,16} colorimetric^{17,18} and electrochemical methods.¹⁹ A few methods
52 have also been reported for the fluorimetric determination of cyanide using QDs.^{20–24}

53 Among these, fluorescent sensors enjoy many advantages. They are highly sensitive,
54 inexpensive, easy to use, and especially suitable as a diagnostic device for analytical
55 purposes. Moreover, they can be employ hands-free via remote controlling.

56 Quantum dots based on organic dyes as fluorophore have attractive properties and
57 several advantages.²⁵ Cyanide could enhance the fluorescence of CdTe QDs, however the
58 linear range was narrow and the selectivity was poor. For resolving this problem, Shang
59 and et al. used copper ion-modified CdTe quantum dots.²⁰ The fluorescence of CdTe QDs
60 was quenched by the copper ions. However, in the presence of CN^- , copper ions could be
61 desorbed from the surface of the QDs and therefore the fluorescence of CdTe QDs
62 increased. In similar report for CN^- detection, copper ion was used as a carbon dot
63 fluorescence quencher.²⁴ Cyanide is well-known to be capable of dissolving nanometals
64 such as Ag in the presence of oxygen and in basic solution.²⁶ In addition the fluorescence
65 of CdTe QDs could be quenched by silver nanoparticles.

66 Here, a novel and simple fluorimetric sensor was reported for cyanide detection
67 based on glutathione-capped cadmium telluride quantum dot (GSH-capped CdTe QDs).
68 One limitation in the fluorescence detection at high fluorescence intensity is self-
69 quenching. In this study, SNPs were used as a quencher to overcome the problem. The
70 method was observed to be highly selective and sensitive for detection of cyanide contents
71 as low as $0.004 \mu\text{g mL}^{-1}$. Moreover, it was found that the detection limit and dynamic
72 range of the proposed sensor was comparable with other fluorescence methods reported in
73 the literature for measuring cyanide (Table 1).

74

75 **2. Experimental**

76 *2.1. Chemicals*

77 Glutathione, sodium tellurite, CdCl_2 and NaBH_4 were purchased from Aldrich. AgNO_3
78 and trisodium citrate were purchased from Merck. All other analytical reagent grade
79 chemicals (with the highest degree of purity available), 0.01 mol L^{-1} carbonate buffer
80 solution and deionized water were used throughout.

81 A $50.0 \mu\text{g mL}^{-1}$ stock solution of cyanide was prepared by dissolving an appropriate
82 amount of NaCN into a 100-mL standard flask.

83 A 0.040 mol L^{-1} CdCl_2 and Na_2TeO_3 (0.010 mol L^{-1}) as precursors were prepared
84 with highest purity available chemicals using deionized water.

85

86 2.2. Apparatus

87 UV-VIS absorption spectra were obtained using a Jasco V-570 UV/Vis/NIR
88 spectrophotometer.

89 The luminescence spectra were measured on a Jasco FP-750 spectrofluorometer.
90 The slit widths of the excitation and emission were fixed at 10.0 nm.

91 Transmission electron microscopy (TEM) experiments were carried out with a
92 Philips CM30 300 kV TEM.

93

94 2.3. Preparation of GSH-capped CdTe QDs

95

96 The GSH-capped CdTe QDs were prepared according to the protocol reported in the
97 literature.²⁷ Briefly, 2.0 mL of 0.04 mol L^{-1} CdCl_2 was diluted to 50 mL. Then, 0.050 g
98 trisodium citrate dihydrate, 0.025 g glutathione, 2.0 mL, 0.010 mol L^{-1} Na_2TeO_3 , and
99 0.025 g NaBH_4 were added to the CdCl_2 solution, while stirring at room temperature.
100 After 2 h, the mixture was refluxed for 12 h at $90 \text{ }^\circ\text{C}$. The resulting solution was
101 transferred to a dark container where it was kept at $4 \text{ }^\circ\text{C}$.

102

103 *2.4. Preparation of citrate-stabilized SNPs*

104 SNPs were prepared via a previously reported method.²⁶ In a brief, 0.125 mL of 0.10 mol
105 L⁻¹ AgNO₃, and 0.125 mL of 0.10 mol L⁻¹ sodium citrate were added to 50 mL of water
106 while stirring continued. Then, 3 mL of a newly prepared 5.0 mmol L⁻¹ NaBH₄ was added
107 into the above aqueous solution and stirred for 30 min. The resulting yellow colloidal
108 SNPs solution was stored at 4 °C overnight before use.

109

110 *2.5. Measurement procedure*

111 For the determination of cyanide, a freshly prepared mixture containing 0.45 nmol
112 L⁻¹ of GSH-capped CdTe QDs and 8.0 nmol L⁻¹ of SNPs, that buffered with the carbonate
113 buffer (pH 10.0), plus an appropriate volume of sample solution were mixed. Then, the
114 fluorescence spectrum of the solution was recorded at 550 – 700 nm upon excitation at
115 400 nm. The slit widths of both the excitation and the emission were set 10.0 nm. The
116 response function (F–F₀) values of the sensor were obtained with different concentration
117 of cyanide, where F and F₀ are the fluorescence intensities at 615 nm in the presence and
118 absence of cyanide, respectively.

119

120 *2.6. Sample preparation*

121 Real samples of human serum and of wastewater were filtered to remove any particles,
122 before analysis. Standard addition method was used for the determination of cyanide. 1.0
123 mL of each real sample (with and without standard solution) was transferred into a vial
124 containing 0.45 nmol L⁻¹ of GSH-capped CdTe QDs and 8.0 nmol L⁻¹ of SNPs at pH 10.0.
125 Then, the fluorescence spectrum was recorded at 550 – 700 nm upon excitation at 400 nm.

126

127 **3. Results and discussion**

128 *3.1. TEM and UV–Vis absorption spectrum*

129 TEM was used to characterize the GSH-capped CdTe QDs and SNPs. The image of the
130 colloidal GSH-capped CdTe QDs solution (Fig. 1A) shows that the nanoparticles are
131 mostly round in shape with an average particle size of ~8 nm. The UV–Vis absorption
132 spectrum of the GSH-capped CdTe QDs (Fig. 2A) shows the wide UV–Vis absorption
133 spectrum as expected of the quantum dots. The spectrum was employed to determine the
134 GSH-capped CdTe QDs content.²⁸ The amount of GSH-capped CdTe QDs was calculated
135 to be 0.34 $\mu\text{mol L}^{-1}$.

136 TEM analysis was also used to verify the size of the SNPs (Fig. 1B). Based on the
137 TEM image of the colloidal SNPs solution, the nanoparticles are mostly round in shape
138 with an average particle size of ~11 nm. The UV–Vis absorption spectrum of the
139 synthesized SNPs is shown in Fig. 2B, as can be seen the wavelength of maximum is ~400
140 nm.

141
142 *3.2. Operating principles*

143 The fluorescence intensity of GSH-capped CdTe QDs was raised in the presence of
144 cyanide. Given the fact that the photoluminescence of QDs arises from electron-hole
145 recombination it is logical to expect that changes in the surface charges or QD
146 components, caused by chemical or physical interactions between ions or small molecules
147 and the QDs, might affect the efficiency of the electron–hole recombination and, thereby,
148 the luminescent emission.²⁹

149 At high cyanide concentrations (above 0.5 $\mu\text{g mL}^{-1}$), the fluorescence intensity of
150 GSH-capped CdTe QDs (in the absence of SNPs) reduces because of the self-absorption
151 effect of GSH-capped CdTe QDs (Fig. 3). In this work, this technical problem (self-
152 absorption) was resolved by adding SNPs.

153 The energy transfer or inner filter effect (IFE) of fluorescence refers to the
154 absorption of the excitation and/or emission of light by absorbers in the detection system.
155 As can be seen in Fig. 2B (from the absorption spectrum of CdTe-QDs and that of SNPs),
156 there is no obvious overlap between the spectrum of CdTe-QDs and that of SNPs.
157 Therefore, it does not reflect the evidence of IFE. But, as can be seen in this figure, the
158 maximum wavelength of SNPs is about 400 nm that is equal to the excitation wavelength
159 of CdTe-QDs. Therefore, the photoluminescence emission intensity of GSH-capped CdTe
160 QDs is reduce in the presence of SNPs. After addition of cyanide ions, the luminescent
161 emission of GSH-capped CdTe QDs was increased. This is due to the fact that in the
162 presence of cyanide, the SNPs is dissolved in the form of $\text{Ag}(\text{CN})_n^{(n-1)-}$, so the plasmon
163 absorption band of the SNPs was decreased²⁶. As evidenced by the absorption
164 spectroscopy (Fig. 4), the absorption band of SNPs decreased gradually.

165 Scheme 1 shows trend of the fluorescence signal of the sensor by addition of cyanide
166 ions. The zeta potential of CdTe-QDs was found to be negative at pH 10. Also, citrate-
167 stabilized SNPs were negatively charged; thus, no obvious interactions (e.g., electrostatic
168 binding) were expected to occur with GSH-capped CdTe QDs. Fig. 5 shows the
169 fluorescence emission spectra of a mixture solution containing different amounts of
170 cyanide (under the optimum conditions). As can be seen in Fig. 5, the proposed sensor
171 works in a 'turn-on' mode, which is generally more sensitive than the turn-off assay mode
172 because the enhanced fluorescence of the signal transduction gives a much better signal-
173 to-noise ratio for the sensing scheme.³⁰

174

175 3.3. Effect of sample solution pH

176 One method most commonly used for dispersing QDs in aqueous solution is to
177 modify their outer surface with anionic carboxylate groups. In this experiment, the

178 fluorescence of the CdTe solution was depended strongly on the solution pH. This means
179 that a suitable buffer should be used to maintain the pH of the aqueous solution at a
180 constant level. For this purpose, the response of the sensor was measured at different pH
181 (6.0–11.0) using solutions containing 0.28 nmol L⁻¹ of GSH-capped CdTe QDs, 8.0 nmol
182 L⁻¹ of SNPs and 1.0 μg mL⁻¹ cyanide (Figs. 6A and 6B). As can be seen, the best pH value
183 for the determination of cyanide by the sensor is 10.0. Since the pK_a of the –COOH group
184 in glutathione is 3.6, the zeta potential of the GSH-capped CdTe QDs is negative at pH
185 10.0. At an adequately basic pH, the electrostatic repulsion between GSH-capped CdTe
186 QDs affords a stable colloidal suspension, whereas an acidic pH yields insoluble
187 aggregates of GSH-capped CdTe QDs.¹ At higher pH levels, however, GSH-capped CdTe
188 QDs may dissolve and the response may also decrease simultaneously at higher pH
189 medium solutions (pH > 10). This is due to the fact that production of too much –OH
190 groups on the surface of QDs hinders cyanide and GSH-capped CdTe QDs interactions.
191 Therefore, pH 10.0 was selected as the optimum pH for further experiments.

192

193 *3.4. Effect of the amount of GSH-capped CdTe QDs*

194 In order to optimize the amount of GSH-capped CdTe QDs in solution, six solutions were
195 prepared with different volumes of GSH-capped CdTe QDs (15 to 50 μL of 34.0 nmol L⁻¹
196 ¹) in the presence of 8.0 nmol L⁻¹ of SNPs and 1.0 μg mL⁻¹ cyanide at pH 10.0. The
197 results are shown in Fig. 7A, clearly confirm that a solution containing 0.45 nmol L⁻¹ of
198 GSH-capped CdTe QDs yields the best response to cyanide. Moreover, the sensitivity of
199 the sensor obviously declines with decreasing the amounts of GSH-capped CdTe QDs. A
200 high GSH-capped CdTe QDs content may lead to the self-absorption of the GSH-capped
201 CdTe QDs fluorescence.

202

203 3.5. Effect of the amount of SNPs

204 SNPs were used to inhibit the self-absorption during fluorescence measurement. The
205 influence of the amount of SNPs on the sensor response was investigated by preparing
206 several solutions with different volumes (25 to 120 μL) of $0.24 \mu\text{mol L}^{-1}$ SNPs in the
207 presence of 0.45 nmol L^{-1} of GSH-capped CdTe QDs and $1.0 \mu\text{g mL}^{-1}$ cyanide at pH 10.0.
208 Based on the results (Fig. 7B), a solution containing 4.0 nmol L^{-1} of SNPs yielded the best
209 response to cyanide. Higher amounts of SNPs were found to lead to reduce the sensor
210 sensitivity.

211

212 4. Analytical figures of merit

213 Under the optimized conditions, the response function ($F-F_0$) values of the sensor were
214 obtained for different cyanide concentrations. Fig. 8 shows the calibration curve under the
215 optimum conditions. The detection limit ($3S_b/m$, where S is the blank standard deviation
216 ($n = 10$), and m is the slope of the calibration curve) was obtained to be $0.004 \mu\text{g mL}^{-1}$.

217 To consider the repeatability of the sensor, 0.5 and $2.0 \mu\text{g mL}^{-1}$ of cyanide solution
218 were measured ten times. The results showed RSD% values of 2.0% and 1.8% for cyanide
219 solutions of 0.5 and $2.0 \mu\text{g mL}^{-1}$, respectively.

220

221 5. Selectivity

222 The potential interference of common anions on the selectivity of the sensor was
223 investigated under the optimum conditions. For this purpose, the optical sensor responses
224 to several anions were examined. The tested anions were including $20.0 \mu\text{g mL}^{-1}$ Br^- , Cl^- ,
225 ClO_3^- , $\text{C}_2\text{O}_4^{2-}$, F^- , I^- , NO_2^- , SO_3^{2-} , SO_4^{2-} , S^{2-} , NO_3^- and SCN^- , and $0.20 \mu\text{g mL}^{-1}$ CN^- . As

226 can be seen in Fig. 9, the proposed sensor exhibits a better selectivity for cyanide than for
227 the other ions examined.

228

229 **6. Application**

230 The applicability of the sensor for real sample analysis was investigated by using the
231 sensor to analyze spiked human serum samples. In addition, to check the accuracy of the
232 sensor, a potentiometric standard method (using CN^- selective electrode) was used to
233 measure the cyanide content in wastewater sample. The results are given in Table 2,
234 confirm the acceptable recovery and accuracy of the sensor.

235

236 **7. Conclusion**

237 A new optical sensor based on GSH-capped CdTe QDs was developed for the detection of
238 cyanide at ultra-trace levels. The fluorescence intensity of the sensor was considerably
239 enhanced in the presence of cyanide. The sensor was capable of determining cyanide
240 content in the range of $0.01 - 2.5 \mu\text{g mL}^{-1}$. The sensor was also found to work in a ‘turn-
241 on’ mode, which is usually more sensitive than a “turn-off” assay. Higher sensitivity,
242 superior selectivity, low detection limit ($0.004 \mu\text{g mL}^{-1}$) and ease of production are the
243 most important advantages of the proposed sensor. Finally, the sensor was successfully
244 employed for the determination of cyanide in real samples.

245

246 *Acknowledgement*

247 The authors wish to thank Isfahan University of Technology (IUT) Research Council
248 and Center of Excellence in Sensor and Green Chemistry for their support.

References

- 1 E. Petryayeva, W.R. Algar, I.L. Medintz, *Appl. Spectr.*, 2013, 67, 215–252.
- 2 A.M. Smith, S. Nie, *Analyst*, 2004, 129, 672–677.
- 3 M.R. Hormozi Nezhad, M.A. Karimi, F. Shahheydari, *Nanotechnology*, 2010, 17, 148–153.
- 4 M.A. El-Sayed, *Acc. Chem. Res.*, 2001, 34, 257–264.
- 5 A.C. Templeton, W.P. Wuelfing, R.W. Murray, *Acc. Chem. Res.*, 2000, 33, 27–36.
- 6 Y. Sun, Y. Xia, *Analyst*, 2003, 128, 686–691.
- 7 A.D. Mc-Farland, R.P. Van Duyne, *Nano Lett.*, 2003, 3, 1057–1062.
- 8 T.R. Jensen, M. Duval Malinsky, C.L. Haynes, R.P. Van Dune, *J. Phys. Chem. B*, 2000, 104, 10549-10556.
- 9 M. Amjadi, J. Hassanzadeh, J. L. Manzoori, *Microchim. Acta*, 2014, 181, 1851-1856.
- 10 The Agency for Toxic Substances and Disease Registry, *Toxicological Profile For Cyanide*, Atlanta, GA, US Department of Health and Human Services, 2006, pp. 221–228
- 11 R. Badugu, J.R. Lakowicz, C.D. Geddes, *Dyes Pigments*, 2005, 64, 49–55.
- 12 C. Lacroix, E. Saussereau, F. Boulanger, J.P. Goullé, *J. Anal. Toxicol.*, 2011, 35, 143–147
- 13 L. Shang, S. Dong, *Anal. Chem.*, 2009, 81, 1465–1470.
- 14 Y. Zhai, L. Jin, P. Wang, S. Dong, *Chem. Commun.*, 2011, 47, 8268–8270.
- 15 Y. Sun, S. Fan, D. Zhao, L. Duan, R. Li, *J. Fluoresc.*, 2013, 23, 1255–1261.
- 16 A.V. Gavrilov, A.A. Druzhinin, K.I. Zakharov, V.A. Ishutin, S.A. Nemkov, I.A. Pushkin, *J. Anal. Chem.*, 2005, 60, 1029–1034.
- 17 A.R. Surleva, G. Drochioiu, *J. Chem. Edu.*, 2013, 90, 1654–1657.
- 18 A.R. Surleva, S. Bancila, E.V. Todorova, *Sci. J. Anal. Chem.*, 2014, 2, 1–6.

- 19 A. Safavi, N. Maleki, H.R. Shahbaazi, *Anal. Chim. Acta* 2004, 503, 213–221.
- 20 L. Shang, L. Zhang, S. Dong, *Analyst* 2009, 134, 107–113.
- 21 W.J. Jin, M.T. Fernandez-Arguelles, J.M. Costa-Fernandez, R. Pereiro, A. Sanz-Medel, *Chem. Commun.*, 2005, 15, 883–885.
- 22 W.J. Jin, J.M. Costa-Fernandez, R. Pereiro, A. Sanz-Medel, *Anal. Chim. Acta*, 2004, 522, 1–8.
- 23 M. Shamsipur, H.R. Rajabi, *Mater. Sci. Eng. C*, 2014, 36, 139–145.
- 24 Y. Dong, R. Wang, W. Tian, Y. Chi, G. Chen, *RSC Adv.*, 2014, 4, 3701–3705.
- 25 U. Resch-Genger, M. Grabolle, S. Cavaliere-Jaricot, R. Nitschke, T. Nann, *NMETH.*, 2008, 5, 763-775.
- 26 L. Shang, C. Qin, L. Jin, L. Wang, S. Dong, *Analyst*, 2009, 134, 1477–1482.
- 27 X. Cui, M. Liu, B. Li, *Analyst* 2012, 137, 3293–3299.
- 28 W.W. Yu, L. Qu, W. Guo, X. Peng, *Chem. Mater.*, 2003, 15, 2854–2860.
- 29 D. E. Moore and K. Patel, *Languor*, 2001, 17, 2541–2544.
- 30 R. Badugu, J. R. Lakowicz and C. D. Geddes, *J. Am. Chem. Soc.*, 2005, 127, 3635–3641

1 Table 1. Comparison of analytical data of fluorescence methods for the determination of
2 cyanide.

Fluorophore	Linear dynamic range ($\mu\text{g mL}^{-1}$)	Detection limit ($\mu\text{g mL}^{-1}$)	Mode of assay	Ref.
Poly[2-methoxy-5-(3,7-dimethyloctyloxy)-1,4-phenylenevinylene]	0.026 – 15.6	0.0156	Enhancement	13
Rhodamine B	0.01 – 3.12	0.001	Enhancement	14
Copper ion-modified CdTe-QD	0.0078 – 0.312	0.0039	Enhancement	20
2-Mercaptoethane sulfonate-modified CdSe-QD	Up to 6.5	0.029	Quenching	21
2-Mercaptoethanol-capped ZnS-QD	0.063 – 0.67	0.0044	Quenching	23
Glutathione-capped CdTe-QD	0.01 – 2.50	0.004	Enhancement	This work

3

4

5

6

7

8

9

10

11 Table 2. Determination of cyanide in real samples.

Samples	CN ⁻ added, ($\mu\text{g mL}^{-1}$)	CN ⁻ found*, proposed sensor ($\mu\text{g mL}^{-1}$)	Recovery (%)	CN ⁻ found*, potentiometric method ($\mu\text{g mL}^{-1}$)
Human serum sample	0.50	0.49 \pm 0.01	98.0	–
	1.50	1.52 \pm 0.03	101.3	–
	2.00	1.97 \pm 0.02	98.5	–
Wastewater	–	2.38 \pm 0.02	–	2.30 \pm 0.13

12 * Average values of six determinations \pm standard deviations.

13

14

15

16

17

18

19

20

21

22

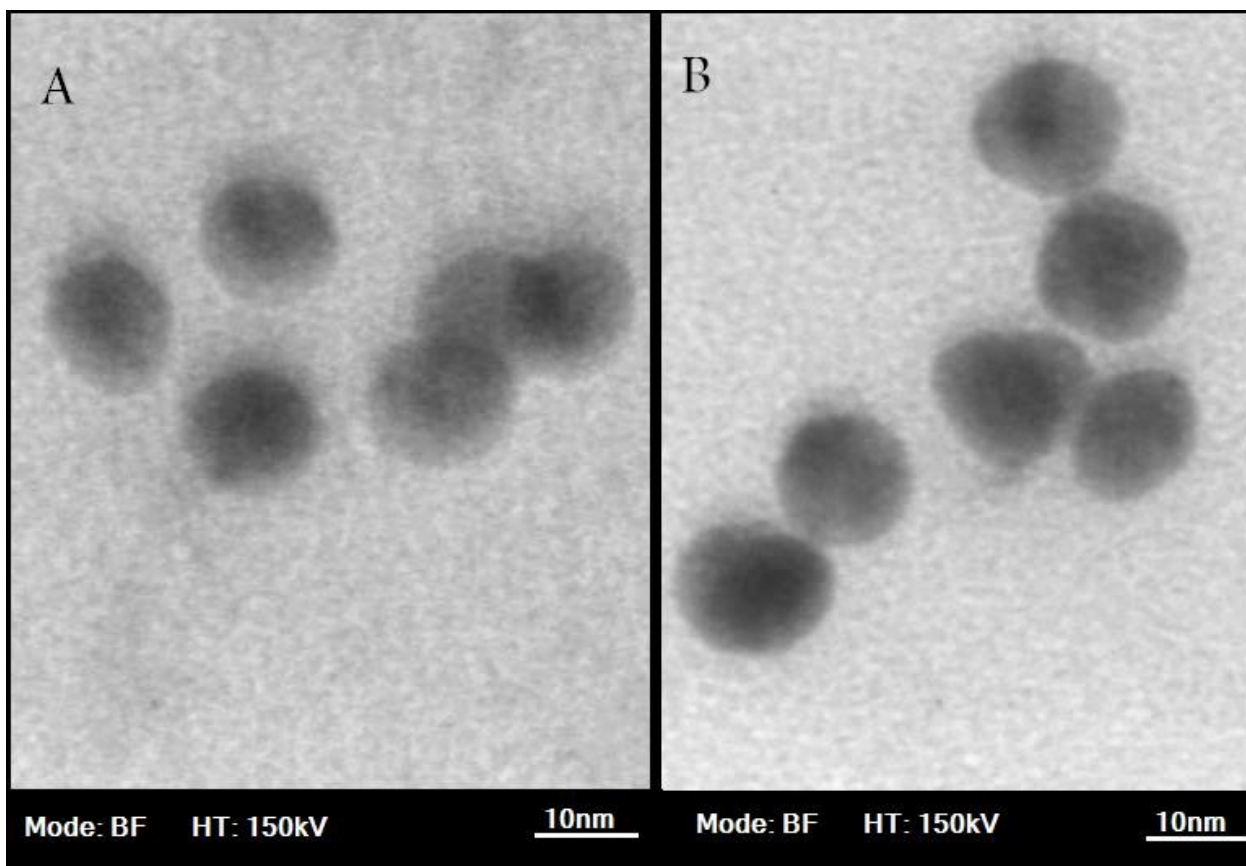
23

24

25

26

27



28

29 Fig. 1. TEM images of applied nanoparticles A): GSH-capped CdTe QDs; and B): SNPs.

30

31

32

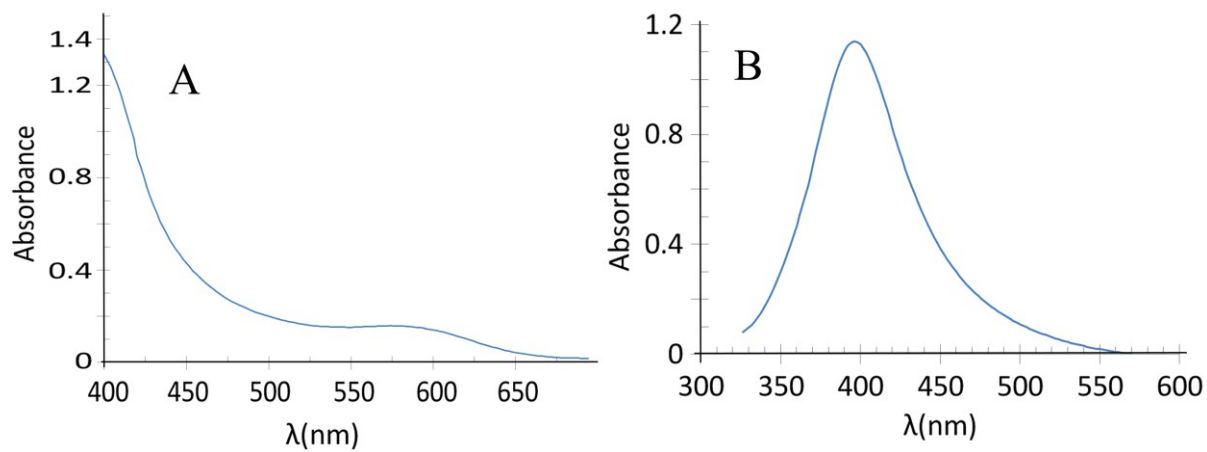
33

34

35

36

37



38

39 Fig. 2. UV-Vis absorption spectrum of prepared nanoparticles A): GSH-capped CdTe

40

QDs; and B): SNPs.

41

42

43

44

45

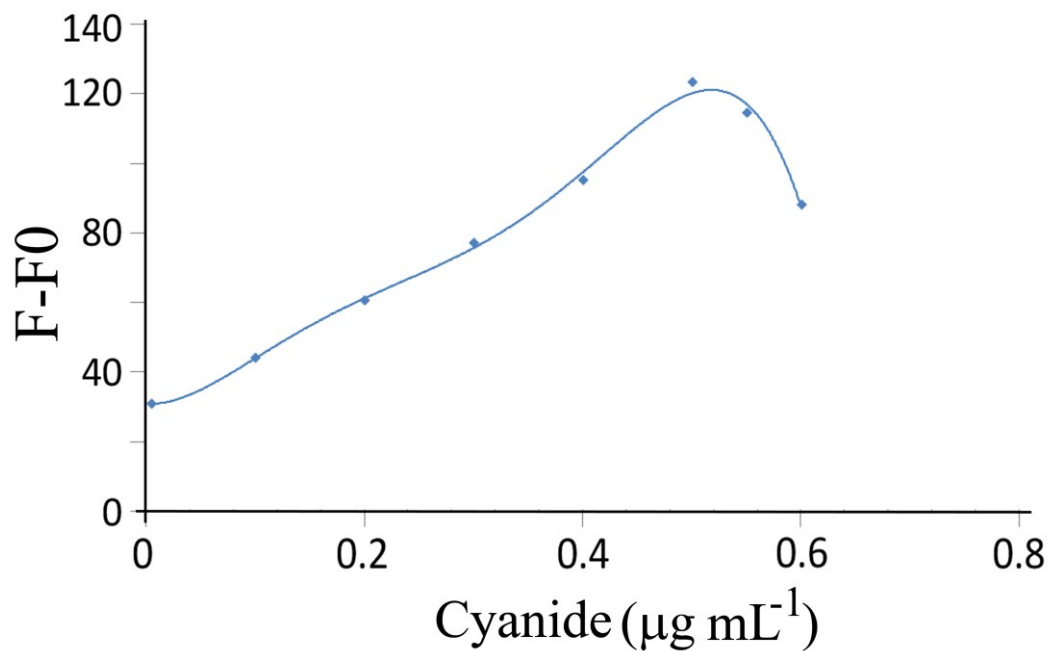
46

47

48

49

50



51

52 Fig. 3. Effect of CN⁻ on the fluorescence intensity of 0.45 nmol L⁻¹ of GSH-capped CdTe

53

QDs at pH 10.0 in the absence of SNPs.

54

55

56

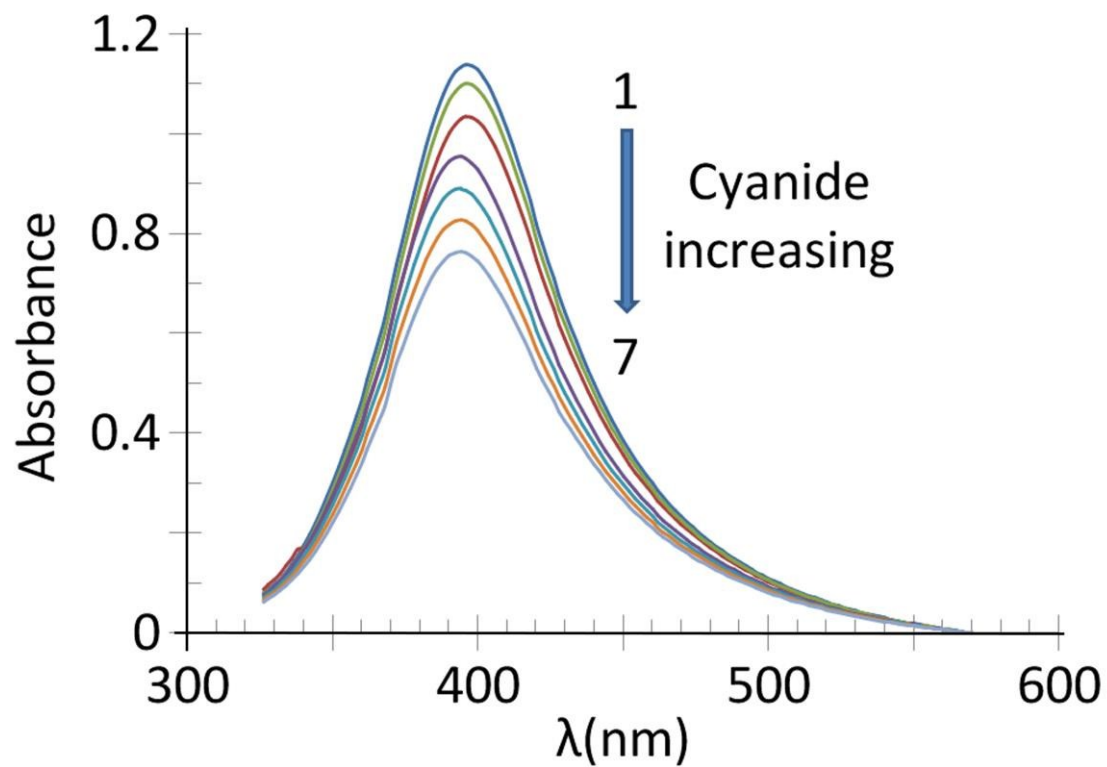
57

58

59

60

61



62

63 Fig. 4. UV-Vis absorption spectra of SNPs at pH 10.0 containing different concentration

64 of cyanide as: 1) 0.00; 2) 0.015; 3) 0.5; 4) 0.15; 5) 1.00; 6) 1.50; 7) 2.00; and 8) 2.50 μg 65 mL^{-1} .

66

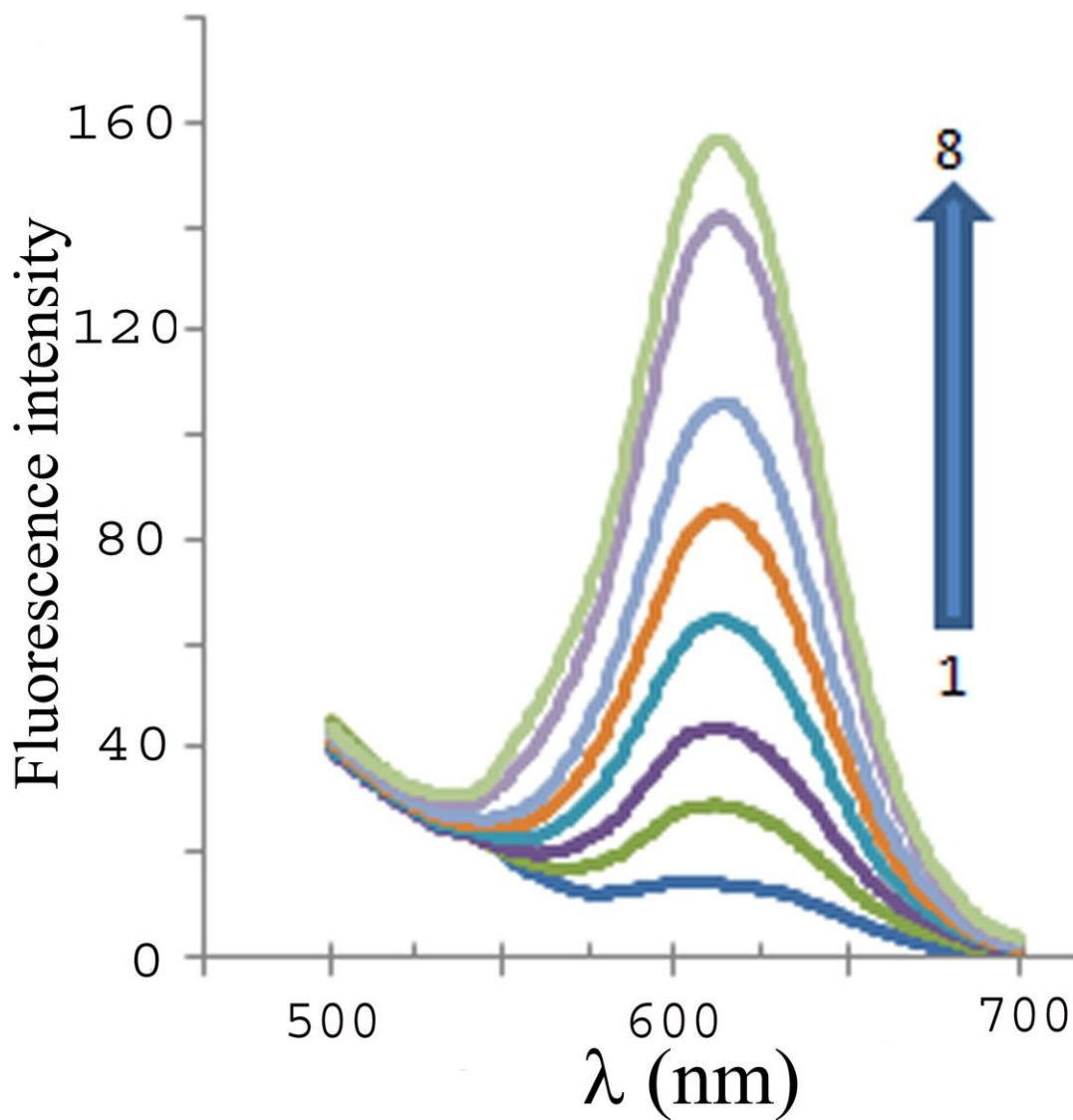
67

68

69

70

71

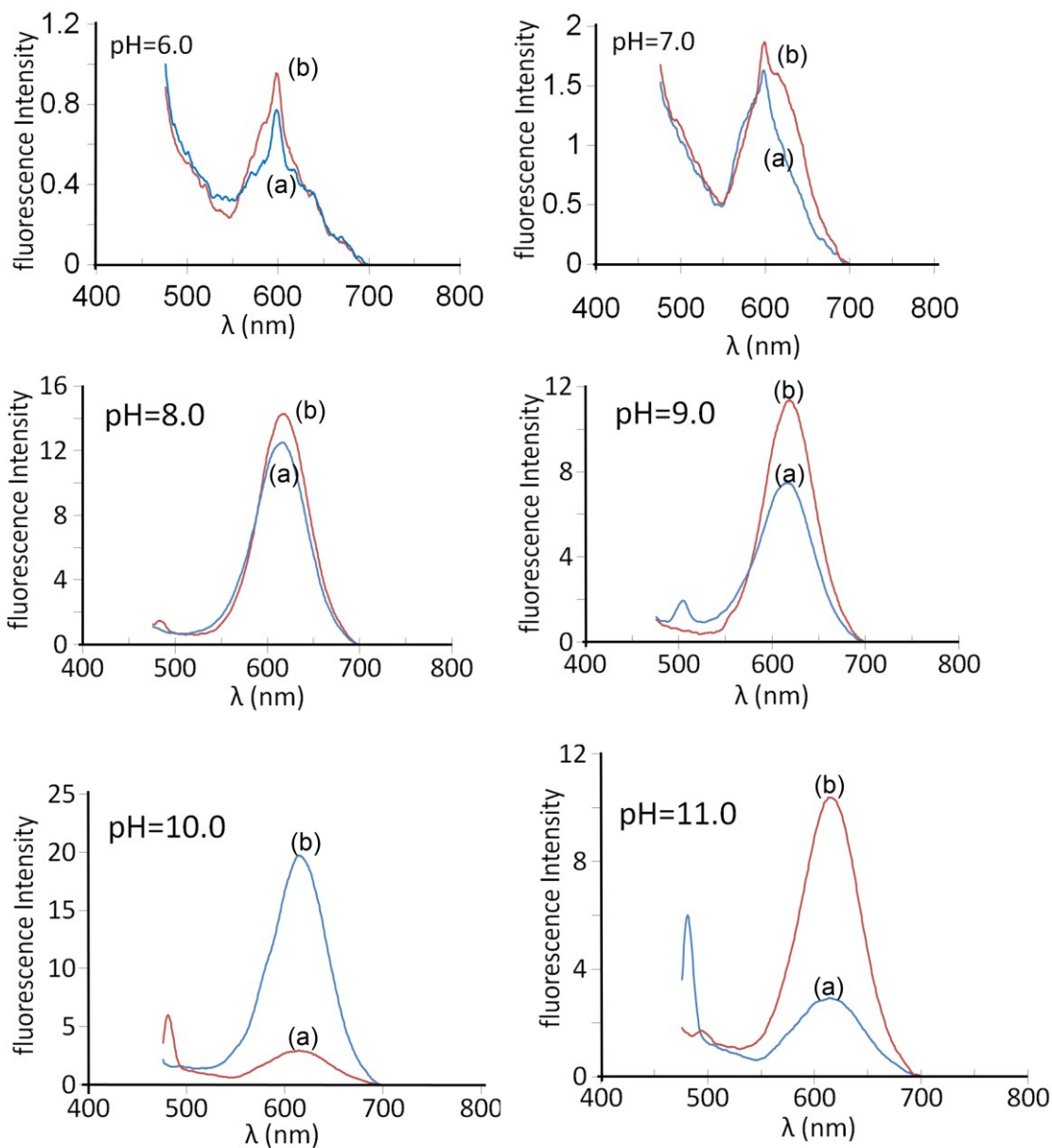


72

73 Fig. 5. Fluorescence spectra of the optical sensor. Conditions: 0.45 nmol L^{-1} of GSH-
74 capped CdTe QDs, 4.0 nmol L^{-1} of SNPs at pH 10.0 containing different concentration of
75 cyanide as: 1) 0.00; 2) 0.01; 3) 0.25; 4) 0.50; 5) 1.00; 6) 1.50; 7) 2.00; and 8) $2.50 \mu\text{g mL}^{-1}$.

76

77

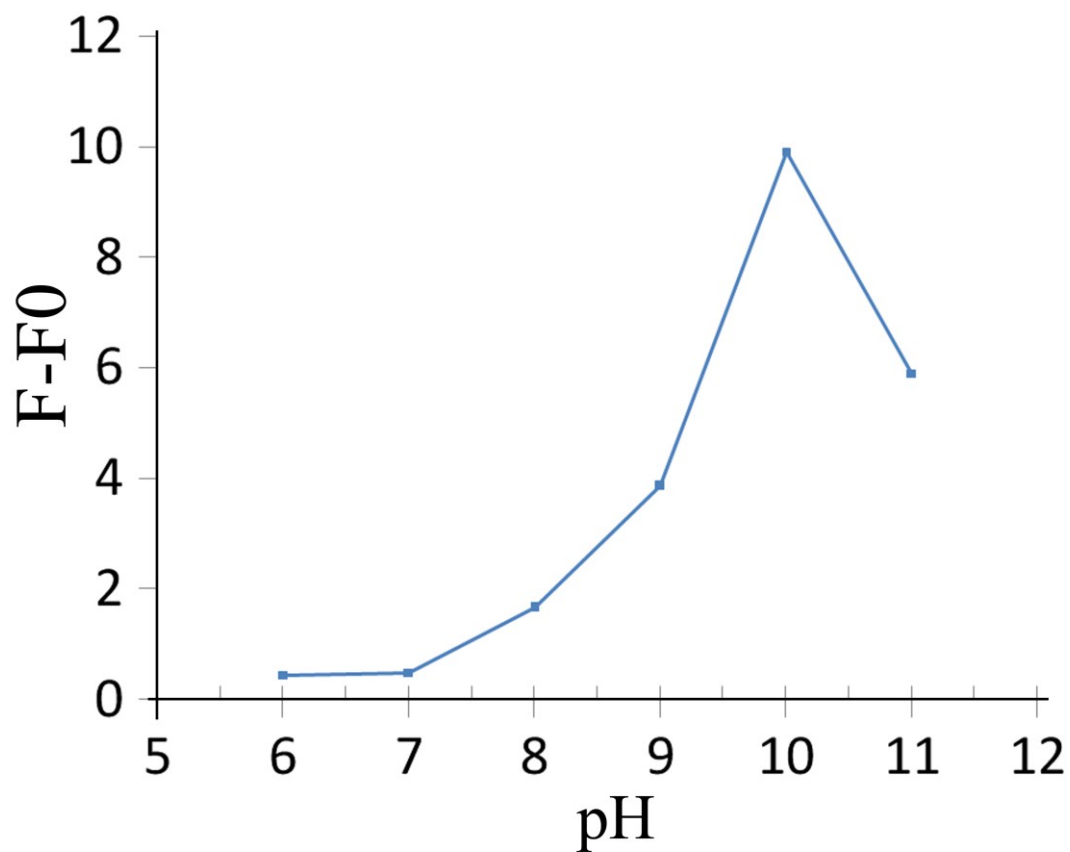


78

79 Fig. 6. A): Fluorescence emission spectra of the blank (a) and sample solutions (b), in the
80 presence of $1.0 \mu\text{g mL}^{-1}$ of cyanide at different pH;

81

82



83

84 Fig. 6B): Diagram of F-F0 vs. the solution pH. Conditions: 0.28 nmol L⁻¹ GSH-capped85 CdTe QDs in the presence of 8.0 nmol L⁻¹ of SNPs.

86

87

88

89

90

91

92

93

94

95

96

97

98

99

100

101

102

103

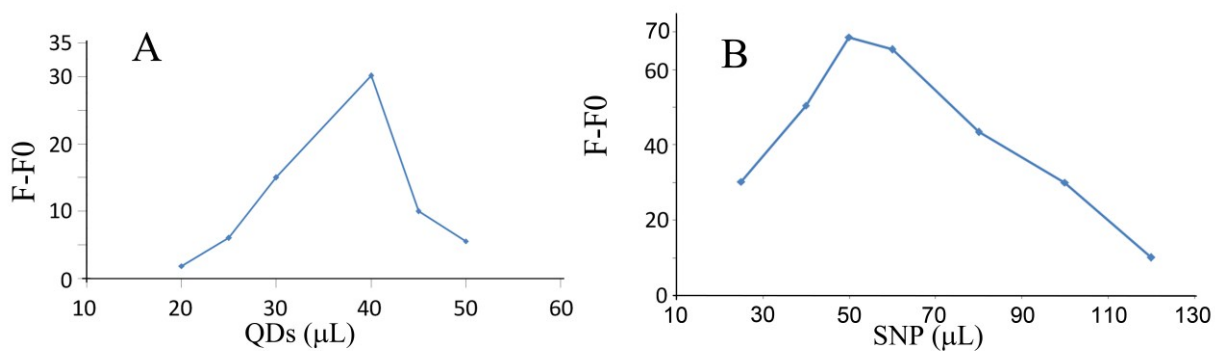
104

105

106

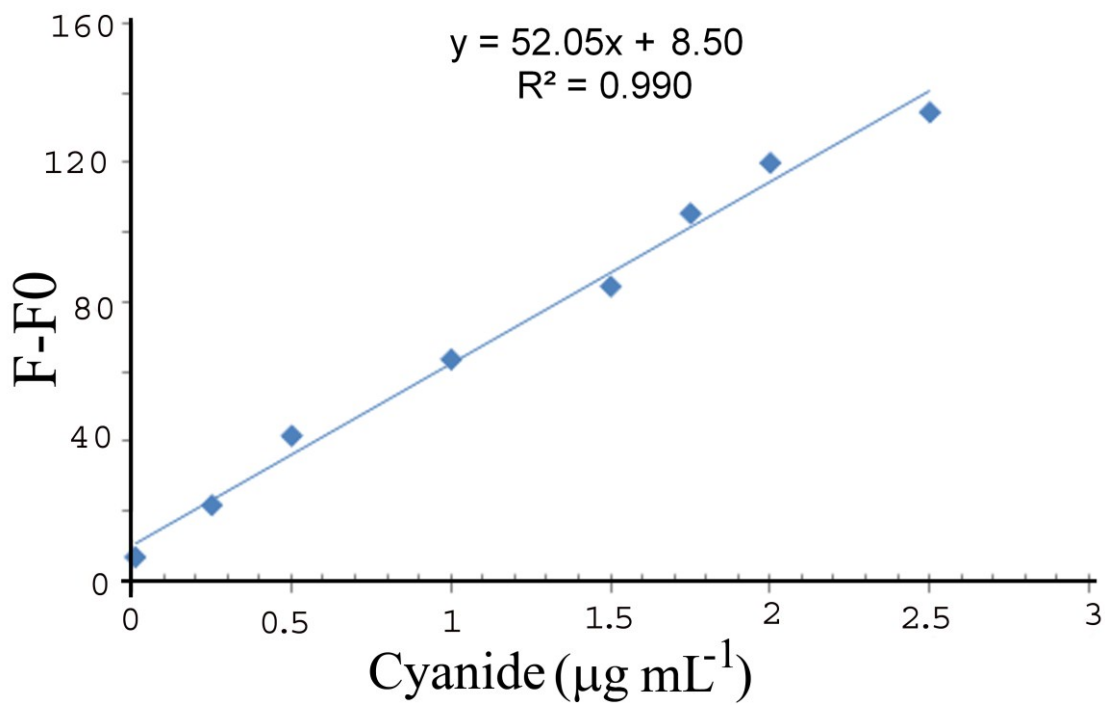
107

108



109
110 Fig. 7. A): Influence of the amount of GSH-capped CdTe QDs on the sensor response to
111 cyanide ions. Conditions: $1.0 \mu\text{g mL}^{-1}$ of cyanide, 8.0 nmol L^{-1} of SNPs, pH 10.0 and
112 different volume of GSH-capped CdTe QDs (34.0 nmol L^{-1}). B): Influence of the amount
113 of SNPs on the response of the sensor to cyanide ions. Conditions: pH, 10.0; $1.0 \mu\text{g mL}^{-1}$
114 of cyanide, 0.45 nmol L^{-1} of GSH-capped CdTe QDs and different volume of SNPs (0.24
115 $\mu\text{mol L}^{-1}$).

109
110
111
112
113
114
115
116
117
118
119
120
121
122
123



124

125 Fig. 8. Calibration graph for the cyanide determination at the optimum conditions.

126 Conditions: pH, 10.0; 0.45 nmol L^{-1} of GSH-capped CdTe QDs and 4.0 nmol L^{-1} SNPs.

127

128

129

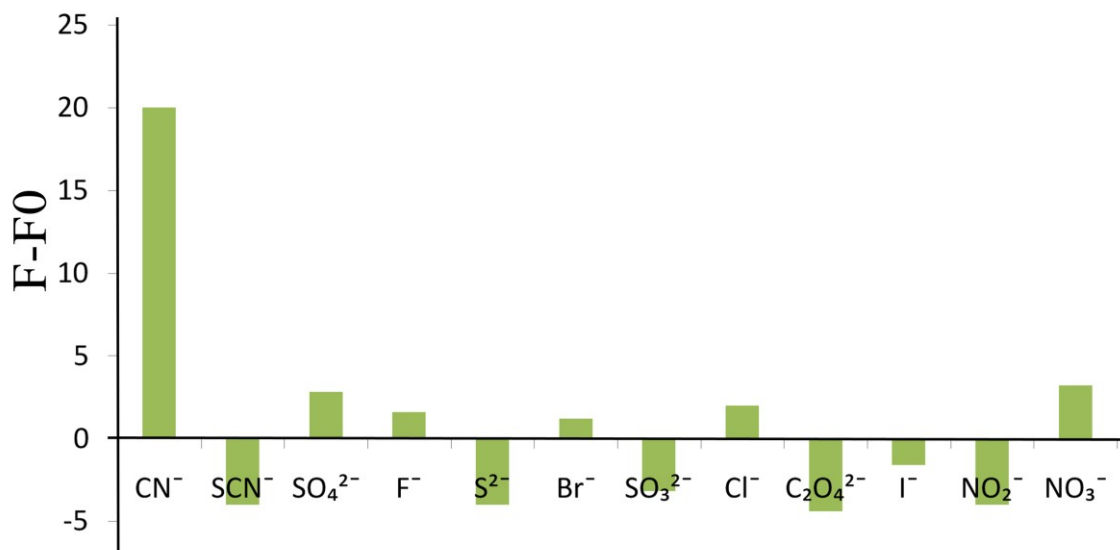
130

131

132

133

134



135

136 Fig. 9. The fluorescence response of a mixture containing 0.45 nmol L⁻¹ of GSH-capped
137 CdTe QDs, 4.0 nmol L⁻¹ of SNPs at pH 10.0 in the presence 0.20 μg mL⁻¹ cyanide and
138 20.0 μg mL⁻¹ of the other anions.

139

140

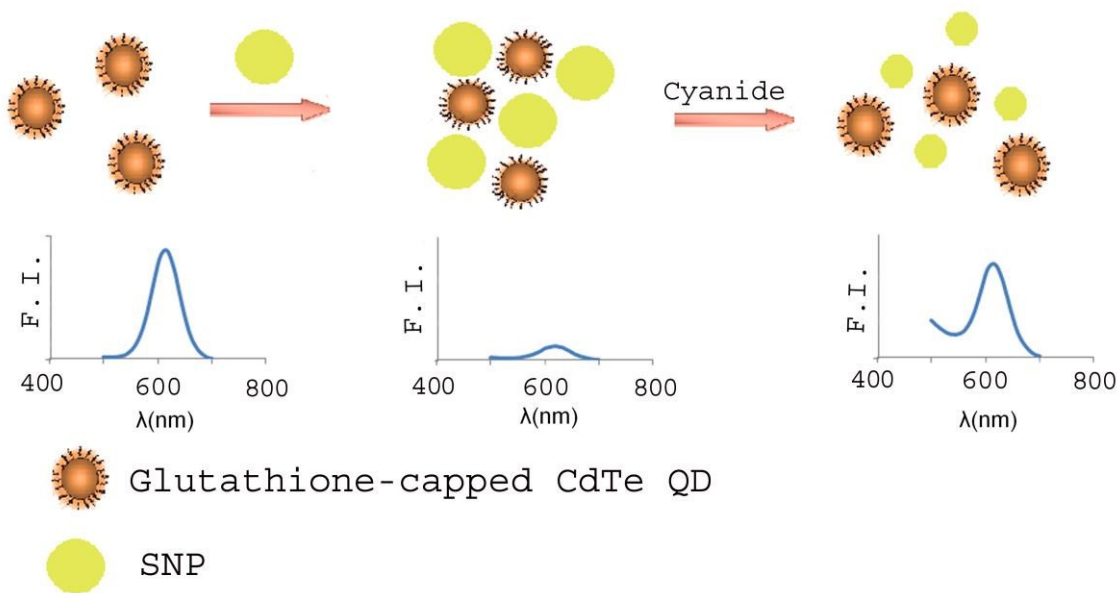
141

142

143

144

145



146

147 Scheme 1. A turn-on fluorescent cyanide sensor based on GSH-capped CdTe QDs using

148 silver nanoparticles.